

## Search for Microbial Signatures within Human and Microbial Calcifications Using Soft X-Ray Spectromicroscopy

Karim Benzerara, Virginia M. Miller, Gerard Barell, Vivek Kumar, Jennyfer Miot, Gordon E. Brown Jr, and John C. Lieske

**Background:** The origin of advanced arterial and renal calcification remains poorly understood. Self-replicating, calcifying entities have been detected and isolated from calcified human tissues, including blood vessels and kidney stones, and are referred to as nanobacteria. However, the microbiologic nature of putative nanobacteria continues to be debated, in part because of the difficulty in discriminating biomineralized microbes from minerals nucleated on anything else (eg, macromolecules, cell membranes). To address this controversy, the use of techniques capable of characterizing the organic and mineral content of these self-replicated structures at the submicrometer scale would be beneficial.

**Methods:** Calcifying gram-negative bacteria (*Caulobacter crescentus*, *Ramlibacter tataouinensis*) used as references and self-replicating calcified nanoparticles cultured from human samples of calcified aneurysms were examined using a scanning transmission x-ray microscope (STXM) at the Advanced Light Source at Lawrence Berkeley National Laboratory. This microscope uses a monochromated and focused synchrotron x-ray beam (80–2,200 eV) to yield microscopic and spectroscopic information on both organic compounds and minerals at the 25 nm scale.

**Results:** High-spatial and energy resolution near-edge x-ray absorption fine structure (NEXAFS) spectra indicative of elemental speciation acquired at the C K-edge, N K-edge, and Ca L<sub>2,3</sub>-edge on a single-cell scale from calcified *C. crescentus* and *R. tataouinensis* displayed unique spectral signatures different from that of nonbiologic hydroxyapatite (Ca<sub>10</sub>(PO<sub>4</sub>)<sub>6</sub>(OH)<sub>2</sub>). Further, preliminary NEXAFS measurements of calcium, carbon, and nitrogen functional groups of cultured calcified nanoparticles from humans revealed evidence of organics, likely peptides or proteins, specifically associated with hydroxyapatite minerals.

**Conclusion:** Using NEXAFS at the 25 nm spatial scale, it is possible to define a biochemical signature for cultured calcified bacteria, including proteins, polysaccharides, nucleic acids, and hydroxyapatite. These preliminary studies suggest that nanoparticles isolated from human samples share spectroscopic characteristics with calcified proteins. However, additional STXM work on these nanoparticles at the N K-edge in particular is needed to determine if they are ~~calcified bacteria or hydroxyapatite nanoparticles that precipitated on proteins.~~

**Key words:** nanobacteria, hydroxyapatite, atherosclerosis, aneurysm, stone formation

---

From the Institut de Minéralogie et de Physique des Milieux Condensés, UMR 7590 and Institut de Physique du Globe de Paris (K.B., J.M.), Paris Cedex, France; Surface and Aqueous Geochemistry Group (K.B., G.E.B.), Department of Geological and Environmental Sciences, Stanford University, Stanford, CA; Departments of Surgery and Physiology and Biomedical Engineering (V.M.M.) and Division of Nephrology (G.B., V.K. J.C.L.), Mayo Clinic College of Medicine, Rochester, MN.

**1** We gratefully acknowledge the support of National Science Foundation Grant CHE-0431425 (Stanford Environmental Molecular Science Institute) (G.E.B.), as well as support from the Stanford Institute for the Environment (G.E.B. and K.B.) and the France-Stanford Center for Interdisciplinary Studies (K.B. and G.E.B.). The work at the Advanced Light Source beam line 11.0.2 was supported in part by the Office of Science, Office of Basic Energy Sciences, Division of

---

Materials Sciences, and Division of Chemical Sciences, Geosciences, and Biosciences of the US Department of Energy at Lawrence Berkeley National Laboratory under contract No. DE-AC03-76SF00098. We acknowledge the support of the National Institutes of Health (DK 62021), The Ralph C. Wilson, Sr., and Ralph C. Wilson, Jr. Medical Research Foundation, and the Mayo Clinic and Foundation.

Presented at Experimental Biology 2006, San Francisco, CA, April 1–5, 2006.

Address correspondence to: Dr. Karim Benzerara, IMPMC, Bat 7, 140 Rue de Lourmel, 75015 Paris, France. e-mail: karim.benzerara@impmc.jussieu.fr.

*Journal of Investigative Medicine* 2006; 54:000–000.

DOI 10.2310/6650.2006.06016

Calcification of arterial tissue is usually considered a strong indicator of chronic inflammatory disease, typically atherosclerosis. Despite its clinical importance, the mechanisms of mineral deposition in arteries are still debated. Nucleation sites facilitating hydroxyapatite (HAP) precipitation are indeed usually needed even under supersaturated conditions, but the nature of such sites is still unclear. Among various hypotheses proposed for pathologic tissue calcification (eg, calcification of mitochondria or of extracellular matrix vesicles), some suggest that microbes can sometimes contribute to such calcification. These hypotheses are based on histologic observations of calcified aortic tissues from patients that sometimes reveal the presence of bacteria.<sup>1</sup> They are also based on many experimental studies that show that some bacterial strains enhance calcium phosphate precipitation partly by promoting crystal nucleation.<sup>2-4</sup>

Folk observed the presence of nanoparticles in natural calcium carbonate deposits by scanning electron microscopy (SEM) and proposed, based only on their morphologies, that they were very small microorganisms, called nanobacteria (NB), that enhanced calcium carbonate precipitation.<sup>5</sup> Several years later, Kajander and Çiftçioğlu reported the isolation of infectious agents of an unusually small size (typically 0.2 to 0.5  $\mu\text{m}$  in diameter, with some even smaller forms of diameter 0.05 to 0.2  $\mu\text{m}$ ) from human and bovine blood and human kidney stones that produced a mineralized outer shell-like structure under physiologic conditions.<sup>6</sup> They observed that when a few drops of this culture were transferred to a fresh medium, precipitation of calcium phosphate occurred in the fresh medium after a few days (ie, transferable biomineralization activity). These nanoforms were characterized by transmission electron microscopy (TEM) and were identified by nucleic acid stains and 16S ribosomal deoxyribonucleic acid (rDNA) sequencing with a sequence ascribed to *Nanobacterium* sp and *Nanobacterium sanguineum*. Since this work, several studies have appeared on this topic supporting the existence of NB and suggesting their involvement in a large number of pathogenesises.<sup>7-11</sup> However, other studies propose an alternative nonmicrobial nature for these calcified nanoparticles. Their small size, which is theoretically too small for viable autonomous life, has been a major argument against them being bacteria.<sup>12</sup> In addition, Cisar and colleagues reported that they were unable to reproduce the microbiology and molecular biology experiments performed by Kajander and Çiftçioğlu<sup>6</sup>; in particular, they noticed that the 16S rDNA sequences were indistinguishable from those of an environmental microorganism that

could have been a contaminant in the polymerase chain reactions.<sup>13</sup> As a result, Cisar and colleagues proposed that the biomineralization processes studied by Kajander and Çiftçioğlu<sup>6</sup> may be attributed to nonliving macromolecules and that nanocrystals of HAP were simply transferred between cultures, resulting in the growth of nanocrystalline HAP in the new culture medium.<sup>13</sup> Based on systematic TEM observations of these nanoparticles and using monoclonal antibodies, Vali and colleagues proposed that NB were actually a novel form of protein-associated mineralization and not living forms per se,<sup>14</sup> which supports the conclusion of Cisar and colleagues.<sup>13</sup>

In our opinion, an insufficient level of characterization of these calcified nanoparticles and the use of nondefinitive criteria for life forms are partly responsible for the ambiguity concerning whether they were microbial organisms. For example, the morphology of calcified nanoparticles, including the description of a purported cell wall-like structure, cannot be used as reliable criteria proving that they are life forms.<sup>15,16</sup> In addition, the effective specificity of various probes used to detect biomolecules can be contested as a definitive criterion.<sup>13</sup> For example, the detection of proteins alone by antibodies does not demonstrate that a nanoparticle is (or once was) a microbial organism.<sup>14</sup> Moreover, fluorescent deoxyribonucleic acid (DNA) probes are detected by optical microscopy, but this method has insufficient spatial resolution to resolve objects smaller than 0.2  $\mu\text{m}$ . As mentioned by Cisar and colleagues, most of the studies of NB ultimately rely on targeting the HAP coatings or some macromolecule labeling and not the organism itself.<sup>13</sup> Here we demonstrate the capacity of scanning transmission x-ray microscopy (STXM) for characterizing directly both the mineral and the organic content of reference bacteria that were experimentally calcified. The objective of this study is to determine if spectroscopic signatures for calcified microbes can be used to decipher the nature of submicrometer-sized calcified particles isolated from pathogenic calcifications. We compare the results with those obtained in our previous STXM study of experimentally calcified *Caulobacter crescentus* cells<sup>17</sup> and study another gram-negative bacterium, *Ramlibacter tataouinensis*, which we calcified in the laboratory<sup>4</sup> and stored in this calcified state for 4 years. These data are compared with STXM data from sphere-shaped particles ranging in size from 30 to 150 nm that were isolated by Miller and colleagues from calcified human aneurysms.<sup>18</sup> This earlier study found that sphere-shaped nanoparticles were transferable (ie, when transferred to a new

medium, calcium phosphate grew in the new medium), stained positively with antibodies, and dyed positively with DNA-specific probes. The researchers also found that the cultures incorporated radiolabeled uridine. These observations provide permissive evidence for the nanoparticles being NB and offer ideal targets for the STXM observations presented in this study.

## Materials and Methods

### Bacterial Cultures in Calcifying Conditions

The calcification medium of *R. tataouinensis* TTB310 was described in Benzerara and colleagues.<sup>4</sup> The strain was kindly provided by T. Heulin (CEA Cadarache, France). *R. tataouinensis* was cultured on 10-fold diluted tryptic soy broth agar medium (TSA/10, Difco Laboratories, agar concentration 15 g/L<sup>-1</sup>) supplemented with CaCl<sub>2</sub> at a final concentration of 10 mM. Owing to the high concentration of phosphates in TSA/10, which buffers the pH to 7.1, the culture medium was highly supersaturated with respect to calcium phosphate phases. To avoid extensive precipitation in the medium, the sterile CaCl<sub>2</sub> solution was added after autoclaving of the TSA/10 medium. Cultures were incubated at 30°C for 3 weeks. One plate dried after several weeks and was kept under ambient conditions for 4 years. Even after this extended period of time, microbial colonies could still be discerned as 1 to 2 mm large yellow calcium phosphate concretions.

### Cultures of Calcified Nanoparticles

Segments of explanted tissue were collected as surgical waste from patients undergoing elective repair of abdominal aortic aneurysm<sup>18</sup> or an S90 nanoparticle culture of bovine origin obtained from Dr. Olavi Kajander (University of Kuopio, Finland). All cultures were maintained in a 150 cm<sup>2</sup> tissue culture flask containing 10 mL of Dulbecco's Minimal Essential Media supplemented with triple-filtered 10% fetal calf serum, 50 μmol/L β-mercaptoethanol, and 3.6 mmol/L CaCl<sub>2</sub>. After 3 weeks, the calcified nanoparticles were washed five times with physiologic buffered saline solution (PBS at pH 7.4), and then the nanoparticles were harvested with a rubber cell-scraper and pooled together in 1.5 mL microtubes for washing, such that each wash consisted of 1 mL PBS centrifugation at 15,000g for 10 minutes. One sample (N1) was the same grid used for TEM experiments in a previous study.<sup>18</sup>

### Sample Preparation for STXM and TEM

Calcified colonies of *R. tataouinensis* were collected from the dried agar plates with tweezers and ground in an agate mortar. The powder was suspended in sterile water, deposited on an Si<sub>3</sub>N<sub>4</sub> STXM sample holder, and dried in air. Liquid suspensions of the human-derived and S90 nanoparticles were washed with a sterile ionic strength buffer (0.01 M NaNO<sub>3</sub>, pH = 7). One drop of each solution was deposited on an Si<sub>3</sub>N<sub>4</sub> STXM sample holder and dried in air. The same sample holders were used in both STXM and TEM studies.

### TEM and STXM Observations

TEM observations were performed on a Jeol 2010F transmission electron microscope operating at 200 kV and equipped with a field emission gun, a high-resolution UHR pole piece, and a Gatan GIF 200 energy filter. GATAN, Inc, Pleasanton CA

STXM characterization studies were performed at the Advanced Light Source (Berkeley, CA) on branch line 11.0.2.2<sup>19</sup> with the synchrotron storage ring operating at 1.9 GeV and 200 to 400 mA stored current. STXM is a type of transmission microscopy using a monochromated x-ray beam produced by synchrotron radiation. The energy of the beam can be varied by increments of less than 0.1 eV over a wide energy range (80–2,200 eV). The beam is focused on the sample using a condenser zone plate down to a spot size of ≈40 nm, which is the spatial resolution achieved in this study. A two-dimensional image is collected by scanning the sample stage at a fixed photon energy. The image contrast results from differential absorption of x-rays, which depends on the chemical composition of the sample. Maps of calcium, nitrogen, and carbon distributions were obtained by subtracting the image below the Ca L<sub>2,3</sub>-edge (≈350 eV) or N (≈400 eV) or C (≈280 eV) K-edge, respectively, from the image of the same area above the edge. Near-edge x-ray absorption fine structure (NEXAFS) spectra were collected at the C K-edge, the N K-edge, and the Ca L<sub>2,3</sub>-edge on calcified *C. crescentus* cells, on *R. tataouinensis* cells, and on calcified nanoparticles isolated from human aneurysms. NEXAFS spectra provide information on the different functional groups present in the selected area for a given element. For example, various functional groups can be discriminated at the C K-edge, including aromatic, ketonic or phenolic, amide, carboxyl, and carbonate groups. Identification of these different functional groups permits discrimination among various biochemical compounds, such as proteins, polysaccharides, or DNA.<sup>4,20,21</sup> AXis2000 software

nucleic acids

[7] (version 2.1n)<sup>22</sup> was used to extract NEXAFS spectra from our measurements. A 150 L/mm grating and 20  $\mu\text{m}$  exit slit were used for carbon K-edge imaging and spectroscopy; a 1,200 L/mm grating and 30  $\mu\text{m}$  slit were used for nitrogen K-edge and calcium  $L_{2,3}$ -edge measurements. Energy calibration was accomplished using the well-resolved 3p Rydberg peak at 294.96 eV of gaseous  $\text{CO}_2$  for the C K-edge, the Rydberg peaks at 406.150 eV and 407.115 eV of gaseous  $\text{N}_2$  for the N K-edge,<sup>23</sup> and the  $L_3$  NEXAFS peak in the calcite Ca L-edge NEXAFS spectrum, which occurs at 349.3 eV.<sup>24</sup>

## Results

STXM capabilities relevant to the search for microbial signatures within calcifications were obtained through the observation of 4-year-old calcified *R. tataouinensis* cells. We know from a previous TEM study that this strain calcifies in less than 3 weeks, with HAP crystals forming in the periplasm and inside the cell.<sup>4</sup> The old samples (4 years after calcification) were used to test the effect of aging on the preservation of the organic content within the calcified cells. The STXM results presented here are very similar to those previously obtained on *C. crescentus* at the C K-edge and at the Ca  $L_{2,3}$ -edges.<sup>17</sup> NEXAFS data at the N K-edge for those two bacteria are also presented.

### STXM Observations of Calcified *R. tataouinensis* Cells at the Ca $L_{2,3}$ -Edge

Figure 1 shows two images of a cluster of calcified *R. tataouinensis* cells taken at a single energy with a spatial resolution of  $\approx 40$  nm, one at an energy below (342 eV, Figure 1A) and one above the edge (349.3 eV, Figure 1B). By converting both images into optical density units and subtracting one from the other, it is possible to obtain an enhanced calcium distribution map (Figure 1C). This energy-filtered imaging procedure is a very useful first step in locating specific calcifications in samples of interest. Moreover, it provides a semiquantitative estimate of the element content as the intensity of each pixel on the distribution map is linearly related to the mass of calcium (ie, the concentration of calcium in the object times the thickness of the object) present in the pixel volume. Hence, it is interesting to note the intensity values provided by the distribution maps for each element to eventually compare them between calcified microbes and calcified nanoparticles. Here, the mean Ca  $L_3$ -edge intensity value for the calcified *R. tataouinensis* cells is 1.8. A Ca  $L_{2,3}$ -edge NEXAFS

spectrum was collected as well on the *R. tataouinensis* cells (Figure 1D). This spectrum is compared with one collected on 3-week-old calcified *C. crescentus* cells and reference abiotic HAP and shows an exact match with the *C. crescentus* spectrum regarding the number, position, and intensity of all the peaks that are at the following energies (see arrows on Figure 1D): 347.1 eV, 347.7 eV, 348.2 eV, 348.6 eV, 349.3 eV, 351.6 eV, and 352.5 eV.

### STXM Observations of Calcified *R. tataouinensis* Cells at the C K-Edge

The same approach as in the Ca  $L_{2,3}$ -edge study was used on the calcified *R. tataouinensis* sample at the C K-edge on the same sample area, and the results are shown in Figure 2. One image was taken at an energy below the C K-edge (280 eV; see Figure 2A) and one was taken above the edge (288.2 eV; see Figure 2B), which corresponds to the maximum absorption energy for various calcified and noncalcified bacterial cells and proteins that were analyzed in previous studies. A difference (distribution) image is shown in Figure 2C, which clearly shows one (and possibly three) *R. tataouinensis* cell(s). The mean intensity value on the *R. tataouinensis* cell displaying the highest contrast is about 0.5. The C K-edge NEXAFS spectrum measured on the calcified *R. tataouinensis* cell displaying the highest contrast showed four prominent peaks at 285.2 eV, 288.2 eV, 289.5 eV, and 290.3 eV and one peak at 286.8, which is barely distinguishable as a shoulder on the peak at 288.2 eV (Figure 2D). This spectrum is compared with spectra collected on (1) 2-day-old noncalcified *C. crescentus* cells, (2) 3-week-old calcified *C. crescentus* cells, (3) noncalcified gram-positive *Bacillus subtilis* cells, and (4) the C K-edge NEXAFS spectra of DNA, albumin taken as a reference for proteins, and calcium carbonate (calcite polymorph). As noted previously,<sup>4</sup> the peak at 290.3 eV could be observed only on calcified bacteria.

### STXM Observations of Calcified *R. tataouinensis* Cells at the N K-Edge

Two images, one below the N K-edge (395 eV; Figure 3A) and one above the N K-edge (410 eV; Figure 3B), were taken on another area of the same sample as discussed above showing two *R. tataouinensis* cells. A mean intensity value of 0.12 was estimated from the difference map (Figure 3C). The N K-edge NEXAFS spectra measured on the *R. tataouinensis* cell located near the top of Figure 3 show<sup>5</sup> three prominent peaks at 399 eV, 399.9 eV, and 401.2 eV (Figure 3D). This spectrum is compared with one collected on 2-

[9]

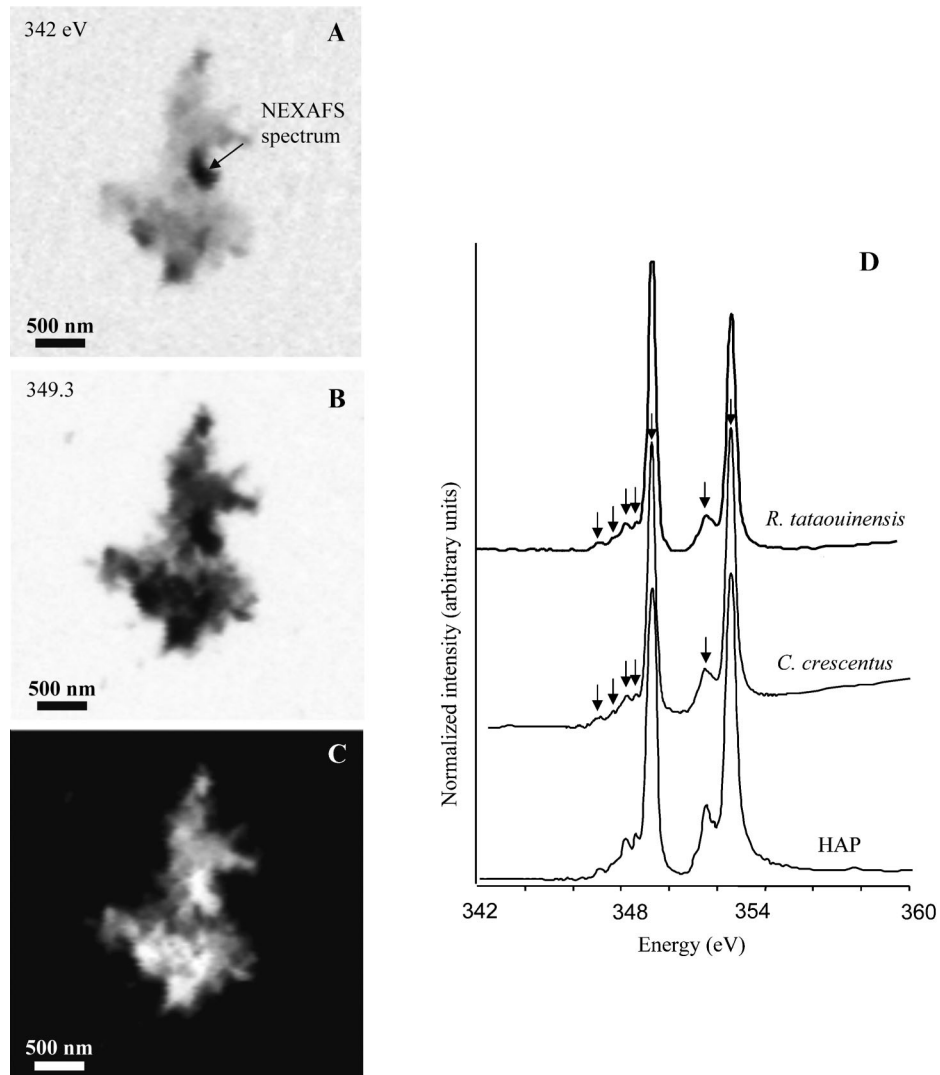


**Figure 1** Spectromicroscopy on calcified *Ramlibacter tataouinensis* cells. *A*, Scanning transmission x-ray microscope (STXM) image of a cluster of *R. tataouinensis* cells (see dark spots marked by arrows) at 342 eV (below the Ca  $L_{2,3}$ -edge). *B*, STXM image of the same area at 349.3 eV, that is, at the  $L_3$  resonance energy. Particles appear to be much darker, showing the presence of calcium. *C*, Calcium map obtained by subtraction of *A* and *B* converted into optical density units. *D*, Calcium  $L_{2,3}$ -edge near-edge x-ray absorption fine structure (NEXAFS) spectra of calcified *R. tataouinensis* cells, *Caulobacter crescentus* cells,<sup>4</sup> and abiotic hydroxyapatite (HAP). The arrows show the different peaks. 8

day-old noncalcified *C. crescentus* cells and one collected on microorganisms entombed in calcium carbonate in a microbialite (Lake Van, Turkey, microbialites; Benzerara and colleagues<sup>25</sup>).

These analyses on reference calcified bacteria provide a framework for subsequent analyses of calcifications that are believed to be involved in pathogenesis. The presence of calcium, carbon, and nitrogen and a semiquantitative estimate of their quantities can be evaluated on submicrometer-sized objects by STXM mapping. NEXAFS spectra at the Ca  $L_{2,3}$ -edges and the C and N K-edges can be

compared with those obtained from the reference calcified bacteria. This comparison is presented in the following section.

#### STXM Observations of Calcified Nanoparticles at the C and N K-Edges and the Ca $L_{2,3}$ -Edge

TEM and STXM observations were combined to characterize three different cultures of calcified nanoparticles: one (named N1 in this study) was used for TEM described by Miller and colleagues<sup>18</sup> and was isolated from calcified abdominal aortic aneurysms; A2 also was isolated from human aneurysm but was

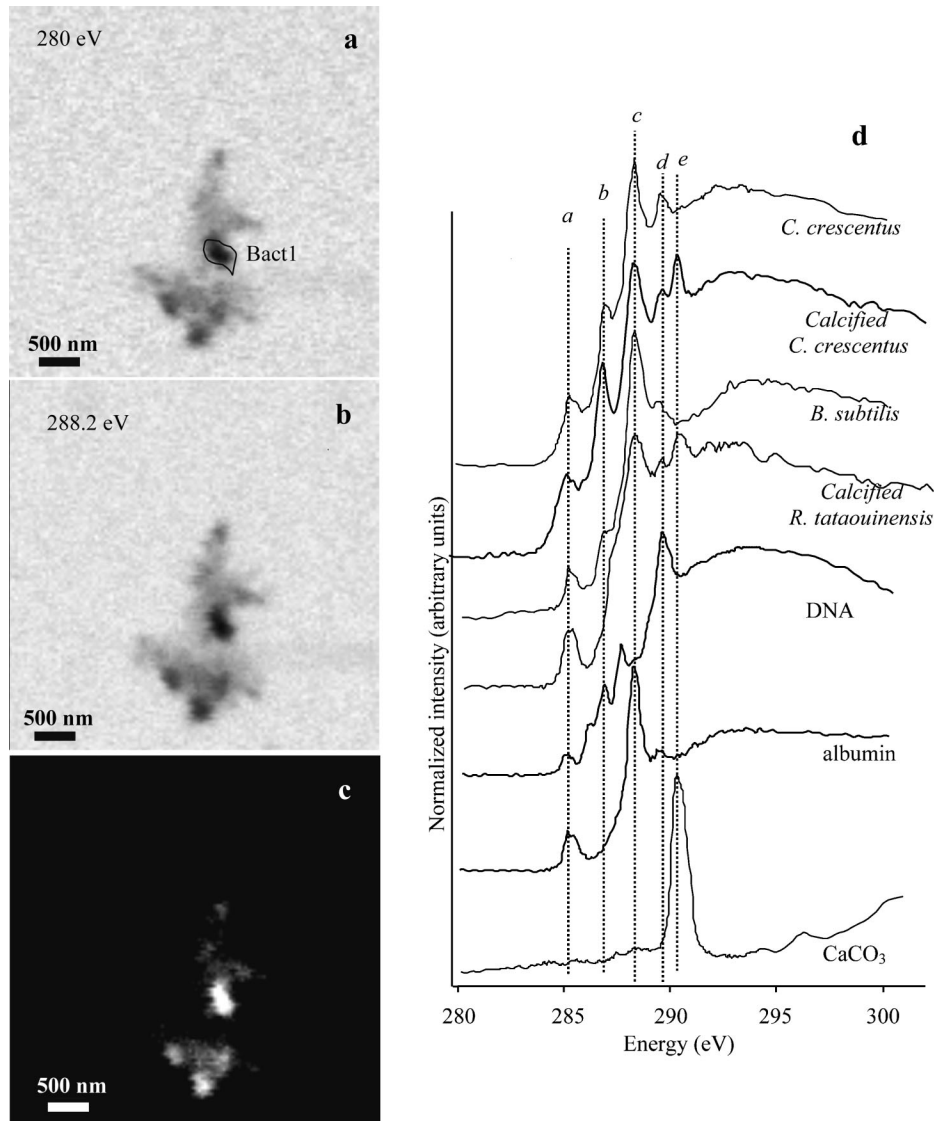


**Figure 2** Spectromicroscopy on the same area as in Figure 1 at the carbon K-edge. *A*, Scanning transmission x-ray microscope (STXM) image taken at 280 eV, below the carbon K-edge. *B*, STXM image taken at 288.2 eV, that is, the resonance energy of carboxylic groups in proteins. *C*, Map of carbon functional groups absorbing at 288.2 eV, that is, mostly proteins, obtained by subtraction of *A* and *B* converted into optical density units. *D*, Carbon K-edge near-edge x-ray absorption fine structure spectra of calcified *Ramlibacter tataouinensis* cells (this study), calcified and noncalcified *Caulobacter crescentus* cells,<sup>4</sup> and noncalcified *Bacillus subtilis* cells. Reference spectra of deoxyribonucleic acid (DNA),<sup>21</sup> albumin (taken as a model for protein; see Lawrence and colleagues<sup>21</sup>), and calcium carbonate (calcite) are shown for comparison. Letters a, b, c, d, and e denote peaks at 285.2, 286.5, 288.2, 289.5, and 290.3 eV, respectively.

prepared as a fresh culture isolate, and S90 nanoparticle cultures were obtained from O. Kajander.

TEM observations show the presence of sub-micrometer-sized calcium phosphate nanoparticles in all of the samples (Figure 4). The texture of the N1 culture (Figure 4, A and B) differs slightly from those of the A2 (Figure 4, C and D) and S90 (Figure 4, E and F) cultures. N1 shows concentric structures that are

reminiscent of cells composed of 80 nm-wide spheres surrounded by clusters of nanocrystals with the same plate-like morphology as usually observed for HAP. The A2 and S90 cultures show 300 nm-wide spheres and rod-shaped forms of the dimensions 120 nm × 350 nm. All of these nanoparticles are composed at least partly of HAP crystals, as shown by EDX analyses and electron diffraction patterns (data not shown).

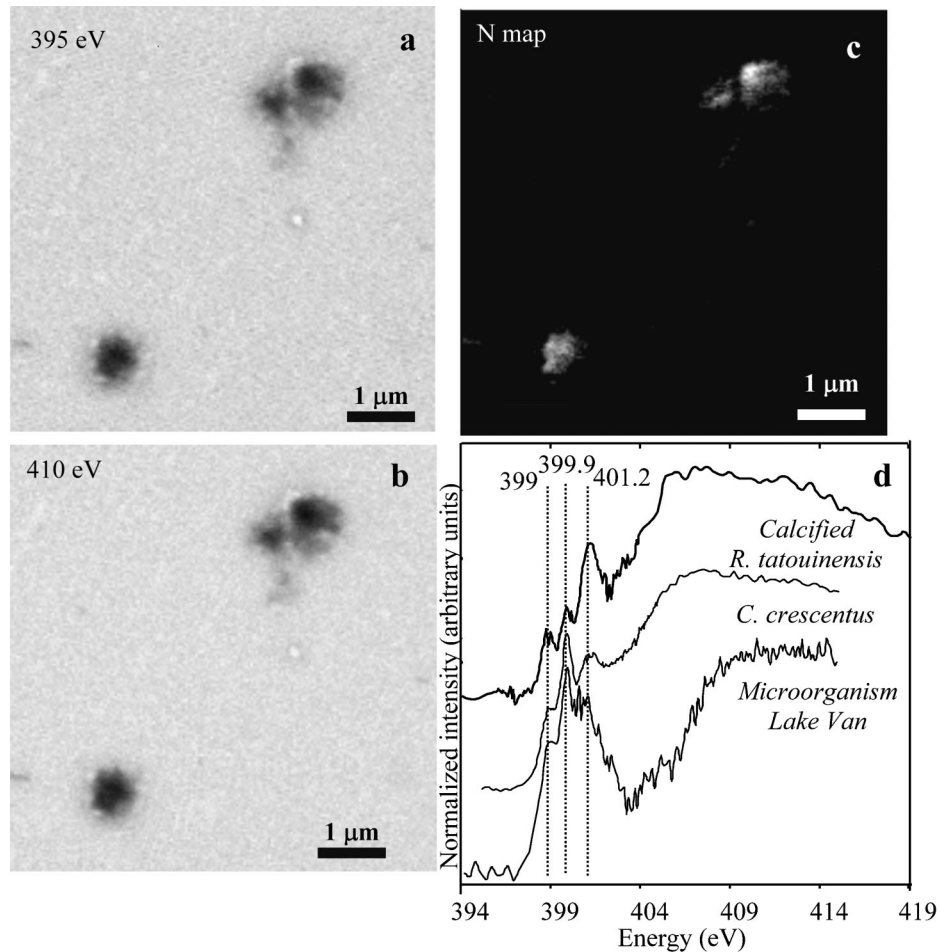


**Figure 3** Spectromicroscopy on calcified *Ramlibacter tataouinensis* cells at the nitrogen K-edge. *A*, Scanning transmission x-ray microscope (STXM) image taken at 395 eV, below the nitrogen K-edge. *B*, STXM image taken at 410 eV, above the nitrogen K edge. *C*, Nitrogen distribution map generated by subtracting *A* and *B*; *D*, Nitrogen K-edge NEXAFS spectra of calcified *R. tataouinensis* cells (this study), noncalcified *C. crescentus* cells,<sup>25</sup> and a microbe entombed in calcium carbonates from a natural environment (Lake Van, Turkey; see Benzerara and colleagues<sup>25</sup>). Vertical dotted lines at 399 eV, 399.9, and 401.2 eV show correlations between the spectra.

The same areas were studied by STXM. Mapping at the Ca L<sub>2,3</sub>-edge supported TEM observations and showed the pervasive presence of calcium on the three sets of samples (the results for S90 are shown in Figure 5). NEXAFS spectra were acquired at the Ca L<sub>2,3</sub>-edge on several calcified nanoparticles from different locations in the three sets of samples. They were all identical and showed the same seven peaks as observed on the NEXAFS spectra measured on calcified bacteria and on abiotic HAP (see Figure 5D).

Mapping at the C K-edge showed the presence of carbon associated with the HAP nanoparticles. Carbon concentrations were much higher in the N1 samples, with intensities on the distribution map up to 0.4 (Figure 6B). Carbon concentrations were, however,

lower in the A2 and S90 samples, with intensities of about 0.07 and 0.03, respectively, as indicated by the distribution maps. NEXAFS spectra at the carbon K-edge were similar for the different samples but with much more noise for A2 and S90, which correlates with the relatively low carbon concentrations in these samples. Three peaks can be easily distinguished at 285.2 eV, 288.2 eV, and 290.3 eV. Peaks at 286.5 eV and 289.5 eV could not be detected in these two samples, however.

Mapping at the N K-edge was performed on the S90 sample. The map distribution showed some particles with intensities up to 0.04. NEXAFS spectra were obtained from such areas and are shown in Figure 7. The spectra are different from N K-edge NEXAFS

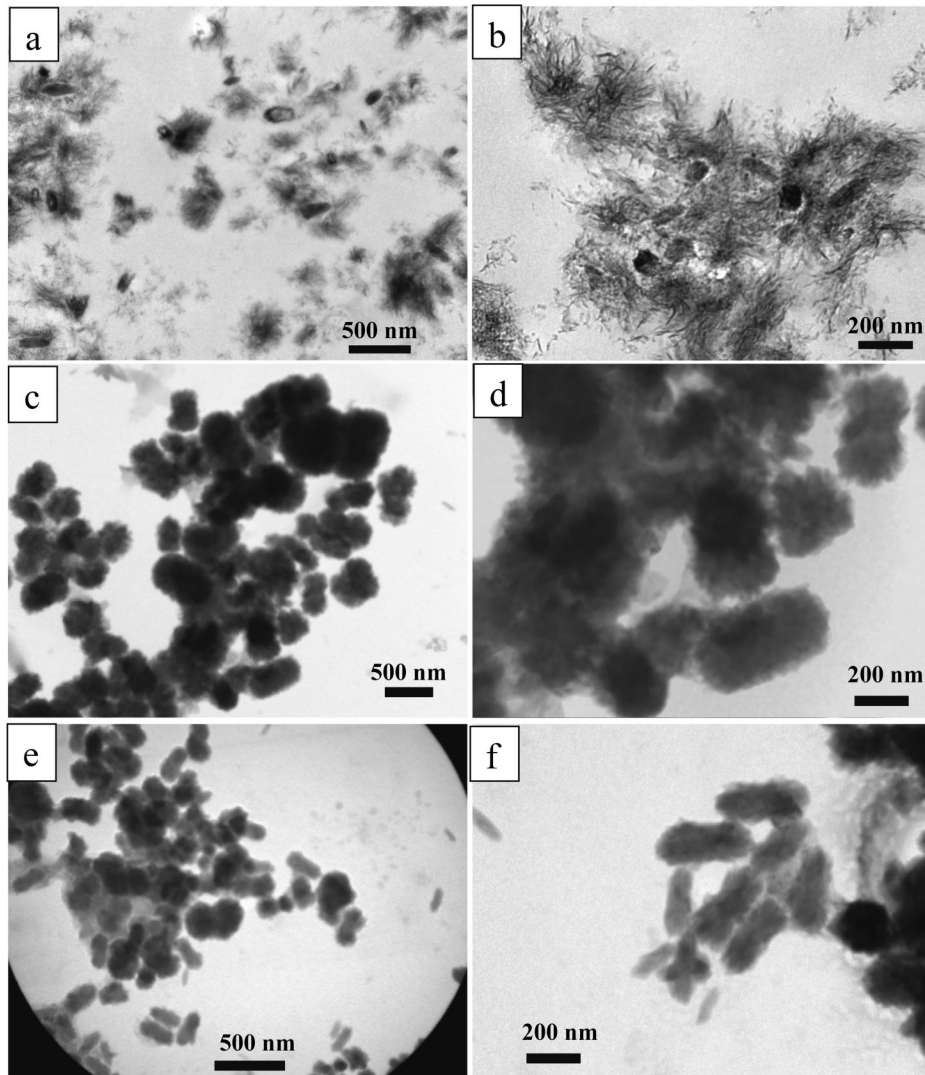


**Figure 4** Transmission electron microscopic images of cultured calcified nanoparticles isolated from human calcifications. A and B are from sample N1; C and D are from sample A2; E and F are from sample S90.

spectra measured on calcified *R. tataouinensis* cells, noncalcified *C. crescentus* cells, or microorganisms from natural environments, with only two pronounced peaks, at 399.8 and 401 eV.

## Discussion

### Spectroscopic Signatures for Calcified Microbes

In a previous study of calcified *C. crescentus* cells,<sup>17</sup> we demonstrated the ability of STXM to provide a good signature for microorganisms versus simple macromolecules such as proteins or polysaccharides. We now have an extended set of data on noncalcified cells, including *C. crescentus*, *B. subtilis*, *Shewanella oneidensis* (data not shown), and the cyanobacteria

*Synechococcus leopoliensis* (data not shown), all of which have identical C K-edge NEXAFS spectra, with four peaks at 285.2, 286.5, 288.2, and 289.5 eV. We also have an extended set of data on calcified cells, including *C. crescentus* and *R. tataouinensis*, which display C K-edge spectra almost identical to those of noncalcified cells except for the presence of an additional peak at 290.3 eV. As explained in Benzerara and colleagues, and in agreement with the indications provided by the NEXAFS spectra at the Ca L<sub>2,3</sub>-edge, which perfectly matches the reference HAP Ca L<sub>2,3</sub>-edge NEXAFS spectrum, it is likely that carbonate groups systematically detected in calcified cells are incorporated into the HAP structure by substitution for phosphate groups and, to a lesser

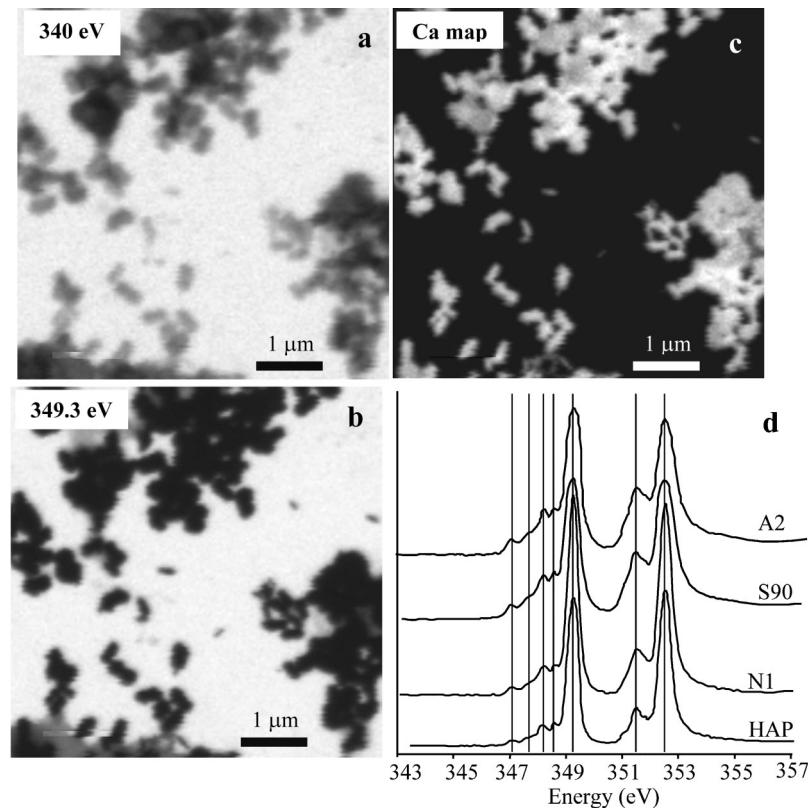


**Figure 5** Spectromicroscopy on cultured calcified nanoparticles isolated from human calcifications at the Ca L<sub>2,3</sub>-edge. *A*, Scanning transmission x-ray microscope (STXM) image of particles from sample S90 at 340 eV (below the Ca L<sub>2,3</sub>-edge). *B*, STXM image of the same area at 349.3 eV, that is, at the L<sub>3</sub> resonance energy. *C*, Calcium distribution map of the same area generated by subtracting *A* and *B*. *D*, Calcium L<sub>2,3</sub>-edge near-edge x-ray absorption fine structure (NEXAFS) spectra of calcified nanoparticles from samples A2, S90, and N1 compared with the NEXAFS spectrum from abiotic hydroxyapatite (HAP).

extent, OH ions, as is usually inferred for HAP.<sup>17,26</sup> Besides, it is postulated that the C K-edge NEXAFS spectra presented in Figure 2 can be used as an empiric but operative spectroscopic signature to detect the presence of microbes in calcifications.

A first step in a less empiric approach, however, consists of identifying the different peaks detected in the NEXAFS spectra. Based on assignments previously made,<sup>20,21,27</sup> peaks at 285.2, 286.5, 288.2, and 290.3 eV can be attributed to aromatic groups, phenolic and/or ketonic groups, peptide bonds, and carbonate groups, respectively. The peak at 289.5 eV is more uncertain but can be tentatively attributed to carbonyl groups. A second step consists of relating these electronic transitions to relevant biomolecules present in bacterial cells. Based on fingerprinting, the 285.2 and 288.2 eV peaks can be tentatively attributed to proteins, whereas the 286.5 eV is usually associated with sugars. The 289.5 eV is at the same energy position as the C = O groups in nucleic acids. From

that perspective, it is worth noting, in agreement with Benzerara and colleagues,<sup>17</sup> that although it may be theoretically possible to design nonmicrobial organic mixtures in the laboratory displaying such a complex spectrum at the C K-edge, we believe that the C K-edge spectrum of bacteria is likely unique and specific and that it is conserved in aged calcified cells.

The N K-edge NEXAFS spectrum of a microbial cell can be discussed in a similar way. Despite variations in relative intensities among the different peaks comprising the N K-edge NEXAFS spectra of calcified versus noncalcified bacterial cells, all of the N K-edge NEXAFS spectra of reference bacteria cells display three peaks at 399, 399.9, and 401.2 eV. The attribution of these peaks to functional groups, however, is much more speculative and will require more work. Based on the N K-edge NEXAFS data presented in Gordon and colleagues,<sup>28</sup> the peak at 401.2 eV can be attributed to amide groups. The peak at 399.9 eV can be related either to heterocyclic

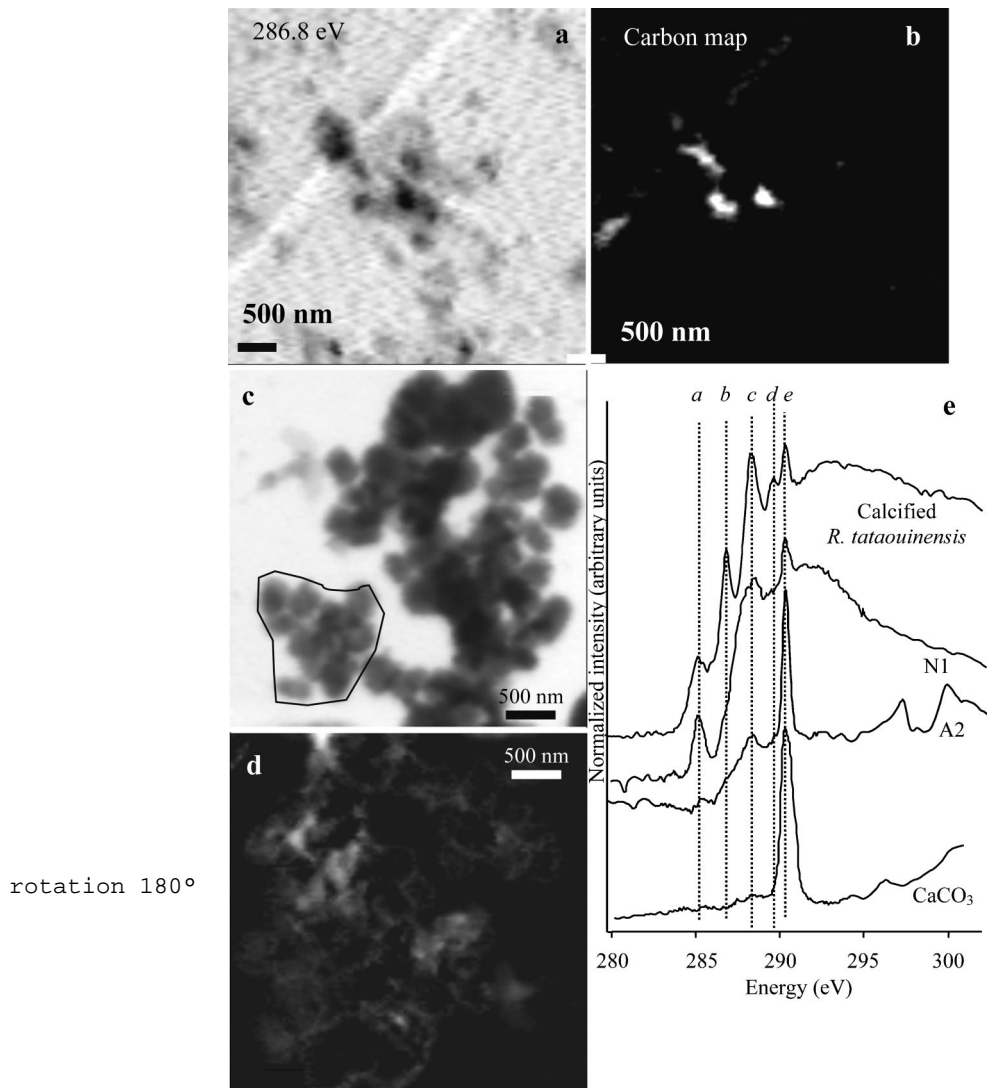


**Figure 6** Spectromicroscopy on cultured calcified self-replicating nanoparticles isolated from human calcifications at the carbon K-edge. *A*, Scanning transmission x-ray microscope (STXM) image on particles from sample N1, taken at 286.8 eV. *B*, Map of carbon functional groups absorbing at 288.2 eV, that is, mostly proteins. *C*, STXM image on particles from sample A2, same area as in Figure 4D, taken at 280 eV. *D*, Map of proteins from the same area. *E*, Carbon K-edge near-edge x-ray absorption fine structure spectra of calcified nanoparticles from samples A2 and N1 compared with a typical spectrum for a calcified *Ramlibacter tataouinensis* cell (this study). A reference spectrum of calcium carbonate (calcite) is shown for comparison. Letters a, b, c, d, and e denote peaks at 285.2, 286.5, 288.2, 289.5, and 290.3 eV, respectively.

aromatics, such as pyridine,<sup>29</sup> which are present in many biologic molecules (eg, nucleic acids, adenosine triphosphate), or to imidazole functional groups, which are present, for example, in histidine.<sup>30</sup> The peak at 399 eV can be attributed to heterocyclic aromatics, such as pyridine.<sup>20</sup> More work is needed to better understand the full information content of the N K-edge NEXAFS spectrum of microbial cells. Until then, the reference spectra shown in this study can be used as empiric spectroscopic signatures.

### Spectroscopic Interpretation of Self-Replicating Calcified Nanoparticles

TEM images taken on the different sets of samples containing calcified nanoparticles show unambiguously that we have observed forms similar to those described in the NB literature, with microbe-like shapes and sizes, although with some exceptions, usually involving sizes less than 200 nm (see Kajander and Ciftcioglu, Cisar and colleagues, Vali and colleagues, and Miller and colleagues<sup>6,13,14,18</sup> for comparisons with Figure 4).

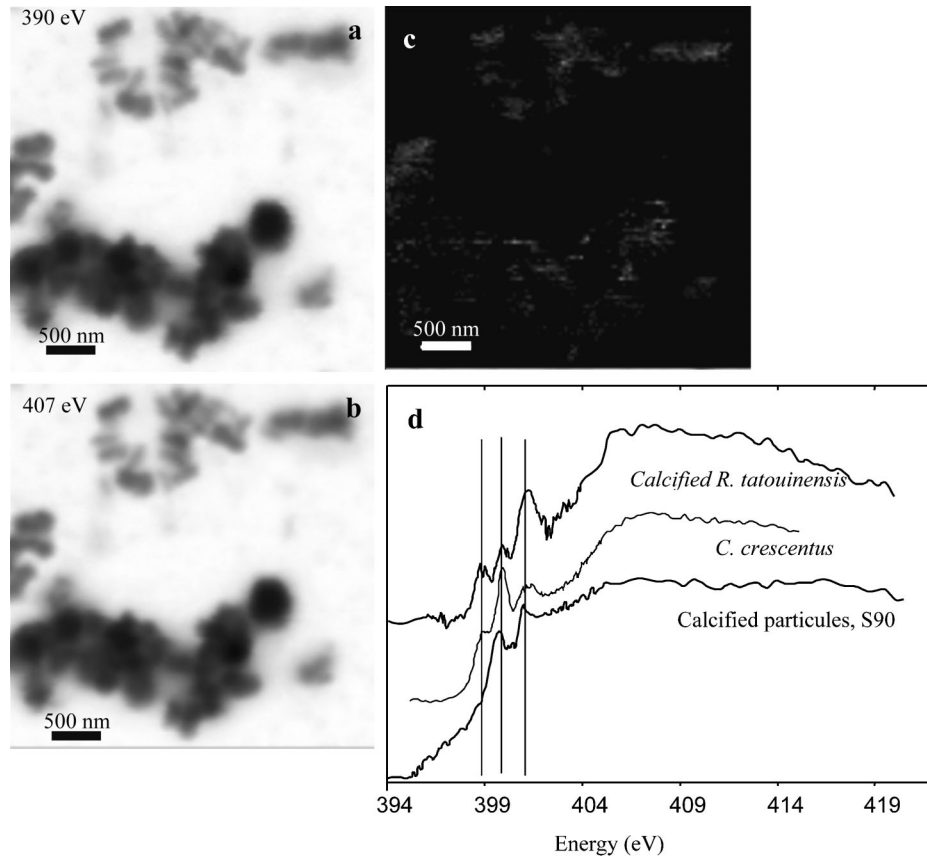


**Figure 7** Spectromicroscopy on cultured calcified self-replicating nanoparticles isolated from human calcifications at the nitrogen K-edge. *A*, Scanning transmission x-ray microscope (STXM) image on particles from sample S90, taken at 390 eV (below the N K-edge). *B*, STXM image of the same area at 407 eV (above the N K-edge). *C*, Map of nitrogen distribution generated by subtracting *A* and *B*; *D*, Nitrogen K-edge near-edge x-ray absorption fine structure spectra of calcified nanoparticles from sample S90 compared with a typical spectrum from a calcified *Ramlibacter tataouinensis* cell (this study) and noncalcified *Caulobacter crescentus* cells. Vertical lines are positioned at 399, 399.9, and 401.2 eV.

NEXAFS spectra at the Ca L<sub>2,3</sub>-edge, electron diffraction patterns, and the systematic detection of a carbonate peak in the C K-edge NEXAFS spectra of the nanoparticles show that carbonate HAP is one of their fundamental constituents, in agreement with previous mineralogic characterizations of these objects.<sup>14</sup> We also found evidence for a carbon- and nitrogen-containing compound almost systematically associated with the nanoparticles. On the basis of NEXAFS spectroscopy at the C and N K-edges, we suggest that this compound is a protein or possibly a mixture of proteins. This suggestion is in agreement with previous studies, which showed staining of the calcified nanoparticles by antibodies and/or extracted candidate protein fractions from them.<sup>6,13,14,18</sup> However, the present study provides the first direct evidence for the presence of proteins in association with these particles, which eliminates potential non-

specific labeling issues. Moreover, based on semiquantitative estimates of carbon and nitrogen contents, we deduce that carbon and nitrogen contents are three to five times lower in the nanoparticles compared with *R. tataouinensis* cells. An exception to this statement is the N1 sample, which displayed a carbon content almost identical to that of *R. tataouinensis* cells. It is more appropriate to compare concentrations, which requires knowledge of the thickness of the sample areas that were probed. Although the anticipated thickness of *R. tataouinensis* is 500 nm, TEM images show that the calcified nanoparticles in the A2 and S90 culture samples have an average thickness of 200 nm. The concentration of proteins may thus be roughly similar for all of these objects. It is not known, however, how aging or the composition of the culture medium might influence protein concentration, which may thus not be diagnostic of microbial cells. It is important to note

that we found no evidence for any protein-rich globules that were not associated with carbonate HAP at the submicrometer scale.

Significantly, we did not detect peaks at the C K-edge in the calcified human nanoparticles other than those unambiguously attributed to proteins and carbonates (285.2, 288.2, and 290.3 eV). In contrast, a number of peaks attributable to a variety of biomolecules were detected in the C K-edge spectra of the reference noncalcified and calcified microbial cells (including peaks at 286.5 and 289.5 eV in addition to those at 285.2, 288.2, and 290.3 eV). Similarly, we did not detect in N K-edge NEXAFS spectra on calcified S90 nanoparticles the peak at 399 eV, which was detected in calcified and noncalcified reference microbial cells. Hence, on an empiric basis, NEXAFS spectroscopy does not support the earlier suggestion that the calcified nanoparticles are calcified bacteria. The NEXAFS spectra of these nanoparticles do not provide evidence for biochemical compounds other than proteins, with the possible exception of the peak at 399.9 eV in the N K-edge spectrum. Additional work is required to understand whether this peak is related to proteins or nucleic acids and whether the nanoparticles are a unique organism distinct from other calcified forms of bacteria we have studied or an interesting example of protein-driven biomineralization.

## Conclusions

STXM offers very useful capabilities for imaging submicrometer-scale organomineral assemblages of interest to the medical sciences. X-ray imaging at the Ca L<sub>2,3</sub>-edge allows quick location of calcified areas in a microbial or human sample. NEXAFS spectroscopy at the C and N K-edges provides signatures for major classes of biochemical compounds (eg, proteins, polysaccharides, nucleic acids) and as proposed in this study a signature for microbial cells. The calcified nanoparticles studied here display C K-edge and N K-edge NEXAFS spectra different from those of reference calcified bacteria. Based on still somewhat limited knowledge of the meaning of these reference NEXAFS spectra, particularly those for nitrogen, we found evidence for the presence of only carbonate HAP and proteins in the calcified nanoparticles. Spectroscopy hence casts doubt on earlier suggestions that these nanoparticles are calcifying bacteria and instead suggests that HAP nanoparticles nucleated and grew in association with a protein matrix in these samples. More work is thus needed to reconcile the biochemical and spectroscopic data on those objects to

determine the true nature of these entities and the forces driving the mineralization. Additional fundamental work is needed to fully deconvolute the NEXAFS spectra from these samples. In any event, the calcified nanoparticles remain a very interesting system to study the process of biomineralization and their mechanism of formation, and the conditions controlling their size and morphology still need to be elucidated. This study also illustrates how STXM can provide an efficient approach to the study of pathogenic calcifications both in vitro and in vivo at the 25 to 40 nm spatial scale with elemental and functional group specificity and thus is complementary to TEM and epifluorescent microscopy.

## Acknowledgments

We wish to thank Tolek Tyliczszak (Advanced Light Source) for his help in optimizing the scanning transmission x-ray microscope on branch line 11.0.2.2 at Advanced Light Source that was used in this study. We also thank Martin Obst and Maria Dittrich for providing samples of *S. leopoliensis* cultures.

## References

1. Ghidoni JJ. Role of *Bartonella henselae* endocarditis in the nucleation of aortic valvular calcification. *Ann Thorac Surg* 2004;77:704–6.
2. Moorer WR, Ten Cate JM, Buijs JF. Calcification of a cariogenic *Streptococcus* and of *Corynebacterium* (*Bacterionoma*) *matruhotii*. *Dent Res* 1993;72:1021–6.
3. Ennever J, Vogel JJ, Streckfuss JL. Calcification by *Escherichia coli*. *J Bacteriol* 1974;119:1061–2.
4. Benzerara K, Menguy N, Guyot F, et al. Biologically controlled precipitation of calcium phosphate by *Ramlibacter tataouinensis*. *EPSL* 2004;228:439–49.
5. Folk RL. SEM imaging of bacteria and nanobacteria in carbonate sediments and rocks. *J Sediment Petrol* 1993;63:990–9.
6. Kajander EO, Ciftcioglu N. Nanobacteria: an alternative mechanism for pathogenic intra- and extracellular calcification and stone formation. *Proc Natl Acad Sci U S A* 1998;95:8274–82.
7. Ciftcioglu N, Bjorklund M, Kuorikoski K, et al. Nanobacteria: an infectious cause for kidney stone formation. *Kidney Int* 1999;56:1893–8.
8. Hjelle JT, Miller-Hjelle MA, Poxton IR, et al. Endotoxin and nanobacteria in polycystic kidney disease. *Kidney Int* 2000;57:2360–74.
9. Hudelist G, Singer CF, Kubista E, et al. Presence of nanobacteria in psammoma bodies of ovarian cancer: evidence for pathogenetic role in intratumoral biomineralization. *Histopathology* 2004;45:633–7.
10. Sommer AP. Could reduced bone mineral densities in HIV be caused by nanobacteria? *J Proteome Res* 2004;3:670–2.

11. Wood HM, Shoskes DA. The role of nanobacteria in urologic disease. *World J Urol* 2006;24:51–4.
12. Neelson KH. Nanobacteria: size limits and evidence. *Science* 1997;276:1776.
13. Cisar JO, Xu DQ, Thompson J, et al. An alternative interpretation of nanobacteria-induced biomineralization. *Proc Natl Acad Sci U S A* 2000;97:11511–5.
14. Vali H, McKee MD, Cifcioglu N, et al. Nanoforms: a new type of protein-associated mineralization. *Geochim Cosmochim Acta* 2001;65:63–74.
15. Benzerara K, Menguy N, Guyot F, et al. Nanobacteria-like calcite single crystals at the surface of the Tataouine meteorite. *Proc Natl Acad Sci U S A* 2003;100:7438–42.
16. Garcia-Ruiz JM, Hyde ST, Carnerup AM, et al. Self-assembled silica-carbonate structures and detection of ancient microfossils. *Science* 2003;302:1194–7.
17. Benzerara K, Yoon TH, Tyliczek T, et al. Scanning transmission x-ray microscopy study of microbial calcification. *Geobiology* 2004;2:249–59.
18. Miller VM, Rodgers G, Charlesworth JA, et al. Evidence of nanobacterial-like structures in calcified human arteries and cardiac valves. *Am J Physiol Heart Circ* 2004;287:H1115–24.
19. Bluhm H, Andersson K, Araki T, et al. Soft x-ray microscopy and spectroscopy at the molecular environmental science beamline at the Advanced Light Source. *J Elec Spectr Relat Phenom* 2006;150:86–104.
20. Myneni SCB. Soft x-ray spectroscopy and spectromicroscopy studies of organic molecules in the environment. *Rev Mineral Geochem* 2002;49:485–579.
21. Lawrence JR, Swerhone GDW, Leppard GG, et al. Scanning transmission x-ray, laser scanning, and transmission electron microscopy mapping of the exopolymeric matrix of microbial biofilms. *Appl Environ Microbiol* 2003;69:5543–54.
22. Hitchcock AP. Soft x-ray spectromicroscopy of polymers and biopolymer interfaces. *J Synchrotron Radiat* 2001;8:66–71.
23. Chen CT, Ma Y, Sette F. K-shell photoabsorption of the N<sub>2</sub> molecule. *Physiol Rev A* 1989;40:6737–40.
24. Rieger D, Himpel FJ, Karlsson UO, et al. Electronic-structure of the CaF<sub>2</sub>/Si(111) interface. *Physiol Rev B* 1986;34:7295–306.
25. Benzerara K, Menguy N, López-García P, et al. Nanoscale detection of organic signatures in carbonate microbialites. ~~Submitted~~. *Proc. Natl. Acad. Sci. USA* 2006;103:9440–9445
26. Mathew M, Takagi S. Structure of biological minerals in dental research. *J Res Natl Inst Stand* 2001;106:1035–44.
27. Boese J, Osanna A, Jacobsen C, Kirz J. Carbon edge XANES spectroscopy of amino acids and peptides. *J Electron Spectrosc Relat Phenom* 1997;85:9–15.
28. Gordon ML, Cooper G, Morin C, et al. Inner-shell excitation spectroscopy of the peptide bond: comparison of the C 1s, N 1s and O 1s spectra of glycine, glycyl-glycine, and glycyl-glycyl-glycine. *J Phys Chem A* 2003;107:6144–59.
29. Vairavamurthy A, Wang S. Organic nitrogen in geomacromolecules: insights on speciation and transformation with K-edge XANES spectroscopy. *Environ Sci Technol* 2002;36:3050–6.
30. Zubavichus Y, Shaporenko A, Grunze M, Zharnikov M. Innershell absorption spectroscopy of amino acids at all relevant absorption edges. *J Phys Chem Lett A* 2005;109:6998–7000.